Modelling of energy and exergy analysis of ORC integrated systems in terms of sustainability by applying artificial neural network

Zafer Utlu[1], Mert Tolon[2] and Arif Karabuga[3,*]

[1] *Department of Mechanical Engineering, Halic University, Istanbul 34445, Turkey;*
[2] *Department of Civil Engineering, Istanbul Gedik University, Istanbul 34876, Turkey;*
[3] *Sustainable Energy Systems Application and Research Center, Halic University, Istanbul 34445, Turkey*

Abstract

The present study focuses on the organic Rankine cycle (ORC) integrated into an evacuated tube heat pipe (ETHP), whose systems are an alternative solar energy system to low-efficiency planary collectors. In this work, a detailed thermodynamic and artificial neural network (ANN) analysis was conducted to evaluate the solar energy system. One of the key parameters of sustainable approaches focused on exergy efficiency is application of thermal engineering. In addition to this, sustainable engineering approaches nowadays are a necessity for improving the efficiency of all of the engineering research areas. For this reason, the ANN model is used to forecast different types of energy efficiency problems in thermodynamic literature. The examined system consists of two main parts such as the ETHP system and the ORC system used for thermal energy production. With this system, it is aimed to evaluate energy and exergy analysis results by the ANN method in the case of integrating the ORC system to ETHP, which is one of the planar collectors suitable for the roofs of the buildings. Within the scope of this study, the exergy efficiency was evaluated on the developed ANN algorithm. The effect rates of parameters such as pressure, temperature and ambient temperature affecting the exergy efficiency of ORC integrated ETHP were calculated. Ambient temperature was found to be the most influential parameter on exergy efficiency. The exergy efficiency of the whole system has been calculated as ∼23.39%. The most suitable BPNN architecture for this case study is recurrent networks with dampened feedback (Jordan–Elman nets). The success rate of the developed BPNN model is 95.4%.

Keywords: energy and exergy analysis; sustainability; artificial neural network; ORC system

*Corresponding author:
arif.karabuga@gmail.com

Received 24 January 2020; revised 10 April 2020; editorial decision 13 May 2020; accepted 13 May 2020

1. INTRODUCTION

Global energy and climate problems arise due to the increase in energy consumption, the decrease in the life of fossil fuels, and the inevitable increase in environmental pollution. According to the World Bank report, energy consumption from fossil fuels has declined dramatically after 1970, but today energy consumption from fossil fuels is still nearly 80% [1–3]. Global warming and environmental waste problems associated with the consumption of fossil fuels will have an impact over the coming centuries. Restrictions on the use of fossil fuels known to be non-environmental have been adopted and signed by the Kyoto Protocol and the Paris agreement by more than 150 countries. Because of governments having taken a decarbonization policy in energy use, it made it necessary to provide alternative solutions to existing fossil resources.

A sustainable structure is the result of a design that focuses on increasing the efficiency of resource use, especially energy. For this reason, it seems very significant to consider sustainable building practices in meeting energy demand. To this end, much effort is

International Journal of Low-Carbon Technologies 2021, 16, 156–164

doi:10.1093/ijlct/ctaa033 Advance Access publication 8 June 2020

being made worldwide to implement renewable energy sources in buildings to use energy efficiently and reduce carbon footprint. Therefore, solar energy systems stand out as applicable in terms of sustainable structures.

For this reason, renewable energy sources have been a rising trend in recent years. Multi-generation (electricity production, hot water use, heating, cooling and clean water production) from solar energy makes solar energy stand out compared to other renewable energy sources [4]. Also, solar-based multi-generation systems reduce carbon-based energy production due to environmental factors and become more attractive for sustainability and applicable to apply at buildings.

As known, solar energy systems can convert solar energy into thermal, mechanical and power energy. According to the International Energy Agency, renewable energy technologies can be divided into three different generations. The first generation is advanced technologies such as hydropower, biomass and geothermal energy. The second generation is the now rapidly developing technologies such as wind, solar and hydrogen energy. The third generation is technologies that are in development, such as concentrated solar energy, ocean energy and integrated energy systems [5]. Evacuated tube heat pipe (ETHP) collectors operate at medium temperature and have better performance than planar solar collectors due to that it can prevent convection and conduction heat losses (because of the vacuum inside the tube) [6, 7]. In ETHP systems, water is generally used as the working fluid for economic purposes. Although water is economical as a working fluid and thermodynamic properties are well known, the most significant disadvantage is that it causes corrosion and freezing of pipes [6,8]. When the current literature on ETHP systems is examined, the researches on this subject are generally focused on experimental studies.

Jowzi *et al*. 2019 [9] analyzed the modified vacuum tube heat pipe system. In this study, both the thermal performance of the system and CFD modeling was performed. At the end of the study, the thermal efficiency of a typical evacuated tube solar collector system was increased by 25% compared to the thermal efficiency of the modified system. Elsheniti *et al*. [10] examined the thermal performance of a vacuum tube heat pipe collector at high inlet temperatures. As a result of the study, it is assumed that collector efficiency decreases at higher inlet temperatures and more series-connected tubes. Ghritlahre and Prasad [11] evaluated the application of the ANN technique to predict the performance of solar collector systems. The evaluations presented in this study show that the ANN technique is a very suitable tool for estimating the performance of solar collector systems. Daghigh and Zandi [12] studied the vacuum tube heat pipe system supported by nanofluids and the auxiliary gas system. In this study, a hybrid solar–gas system was designed and manufactured. MWCNT, CuO and TiO_2 nanofluids have higher performance than water. MWCNT, CuO and TiO_2 nanofluid efficiencies increased by 25, 12 and 10% in August and 25, 15 and 7% in October respectively.

Jayanthi *et al*. [13] have examined the thermal performance analysis of heat pipe solar collectors. In this study, they set up an experiment set using four pipes with a length of 1800 mm and a diameter of 58 mm. They used R134a as a working fluid. The efficiency of the solar collector was found to range from 31.28 to 42.95%. Li *et al*. [14] have conducted a numerical and theoretical analysis of a vacuum tube thermal tube system. They performed numerical simulation at different flow rates. A conceptual model of secondary flow was established to estimate flow and temperature distribution. Compared with the existing model, the developed model has more accurate results in determining flow and temperature distribution. Hojjat [15] has developed an ANN model to predict the thermal and hydrodynamic behaviour of two different Newtonian nanofluids used as refrigerants in two different heat exchangers. As a result of the study, it was found that the ANN model established predicts the experimental study results with high accuracy. Daniels *et al*. [16] have studied an ETHP solar energy system experimentally to melt snow on the sidewalk in winter. In the study on a 3.05 m × 1.22 m × 0.13 m plate, 2°C temperature was obtained, and snowing on the plate was prevented. The ETHP system collected an average of 2.7 kW of power per day. Iranmanesh *et al*. [17] have investigated the performance of an ETHP system with PCM and solar cabinet drying system. As a result of thermal analysis, they found that using PCM increased the input heat energy between 1.72 and 5.22% for 0.025 and 0.05 kg/s airflow, respectively.

Tolon *et al*. [18] have presented ANN modeling of an ETHP system. In the study, the ANN model is established by handling 220 data. As a result of the study, the highest exergy efficiency is calculated as 33.57% in the case of a mass flow of 0.01 kg/h. Shahverdi *et al*. [19] have made numerical modeling of the organic Rankine cycle (ORC) system connected to a parabolic solar collector. Two different absorber tubes and seven different fluids are used for the ORC system. As a result of the study, the highest net power obtained from the ORC system has provided using R113 fluid. Facão *et al*. [20] have investigated a micro-cogeneration system that produces 5 kW in three different countries, such as Spain, Tunisia and Egypt. The ORC system operates between 80, 100–150 and 200–250°C temperatures. They used two fluids, such as cyclohexane and R245fa, in the system. Jradi *et al*. [21] have presented a micro scale cogeneration system using a novel scroll expander. In the study, the energy source of the system is solar biomass-assisted. Also, in the system, they used HFE-7100 as a working fluid. They calculated maximum electric power production of 500 W in the expander, in case of the under-pressure of 4.5 bars. Wei *et al*. [22] have presented an electric generation system at low temperature by ORC assistance. Besides, they have used R152a as a working fluid in the system. The energy and exergy efficiencies calculated in the study is 5.02 and 26.5% when the temperatures of the heat source and cooling source are 65 and 11°C, respectively. Selbas and Yilmaz [23] have investigated the thermodynamic analysis of the solar-assisted ORC system. In this study, they used R410a as the working fluid. In the result of this study, they have calculated energy and exergy efficiencies of whole system as 10.6 and 69.2%, respectively. Also, they found an evaporation pressure essential effect on efficiencies.

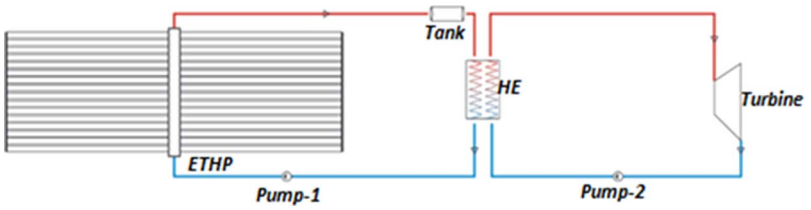

Figure 1. *The schematic diagram of the evacuated tube heat pipe (ETHP) system.*

When the literature study is analysed, they generally performed energy and exergy or performance analysis of solar-based multiple generation systems and different types of solar energy systems. The difference between this study and other studies is that ANN modeling is done in addition to the energy and exergy analysis of the ETHP system. This showed that the BPNN model installed had the highest success rate for the ETHP-based ORC integrated system.

This study aims to integrate the artificial neural network (ANN) system to the calculations of the exergy efficiency of the experimentally installed evacuated tube heat pipe collector's ORC system. At the end of the study, the effect rates of parameters such as temperature, mass and radiation on system efficiency were calculated. The main objectives and the contribution to the literature of this study are as follows.

- To perform an extensive thermodynamic analysis of the ETHC solar system
- To perform ANN modeling of the ETHP system
- To make energy and exergy analysis by integrating the ORC system to the ETHP system
- To conduct ANN modeling to determine the effective parameters on the exergy efficiency of the ORC-integrated ETHP system
- To investigate the sustainability of an ETHP based electricity generation system

2. MATERIAL AND METHODS

This section consists of a solar-based power generation system description, the parameters affecting the exergy efficiencies of both the ETHP system and the ORC system in terms of thermodynamic analysis and construction of ANN architecture.

2.1. ETHP system description

Planar collectors can be thought of as a kind of energy converter so that the solar radiation from the sun converts the energy into thermal energy. The radiation energy from the sun is absorbed by the collector and transfers the obtained thermal energy to the working fluid (such as air, water, thermal oil and refrigerant) [24]. The ETHP system consists of an evacuated tube heat pipe collector, a hot storage tank, two circulating pumps, a heat exchanger and an ORC turbine. A schematic diagram of the complete ETHP is illustrated in Figure 1. The analysis of the evacuated tube heat pipe (ETHP) system is based on the following main assumptions:

- The system works under steady-state conditions.
- The changes in kinetic and potential energies are neglected.
- The pressure drops and heat losses in the connecting pipes are neglected.
- The compressor works with the adiabatic compression process.
- The system operates at the atmospheric condition of $T_0 = 25°C$ and $P_0 = 1$ bar as the reference state.

T_0 and P_0 are dead state (ambient) temperature and dead state pressure, respectively.

The ETHP system has 108 heat pipes, and each tube consists of two intertwined tubes. The diameter of the outer tube is 47 mm, the outer diameter of the copper tube is 10 mm and the length of the tube is 1800 mm. The copper tube is vacuumed between the glass tube and evacuated between the copper tube and the glass tube. Therefore, the solar radiation coming into the glass pipe is absorbed, and the heat transfers its energy to the water as the working fluid in the pipe, and the rest is emitted again. The thermal energy obtained is transferred to the heat exchanger. By heat exchanger, thermal energy is transferred to the working fluid R134a in the ORC system. The working fluid is heated up to about 85°C with a heat exchanger and passes through to Turbine-I for power generation. A schematic shows the internal structure of ETHP is illustrated in Figures 2 and 3. The shows of the ETHP system is illustrated in Figure 4.

2.2. Thermodynamic analysis

This section focuses on the first and second law analyses of thermodynamics. The energy analysis in a system is used to calculate the amount of energy the process can improve. The energy analysis allows the system to be compared with the most efficient system [25]. Energy analysis is related to the first law of thermodynamics, and it examines the energy balance, energy conservation and energy efficiency of systems. However, energy analysis is not enough to know all aspects of energy use in the system. This is because we cannot calculate the usefulness and quality of energy with the first law. For this reason, to find the real efficiency of the system, exergy analysis, which is related to the second law of thermodynamics, should be done. Exergy analysis calculates exergy losses, exergy destruction and exergy efficiency. Otherwise, exergy is a critical concept to understand the sustainability of energy, environmental effects and utilization of energy well [8, 26, 27].

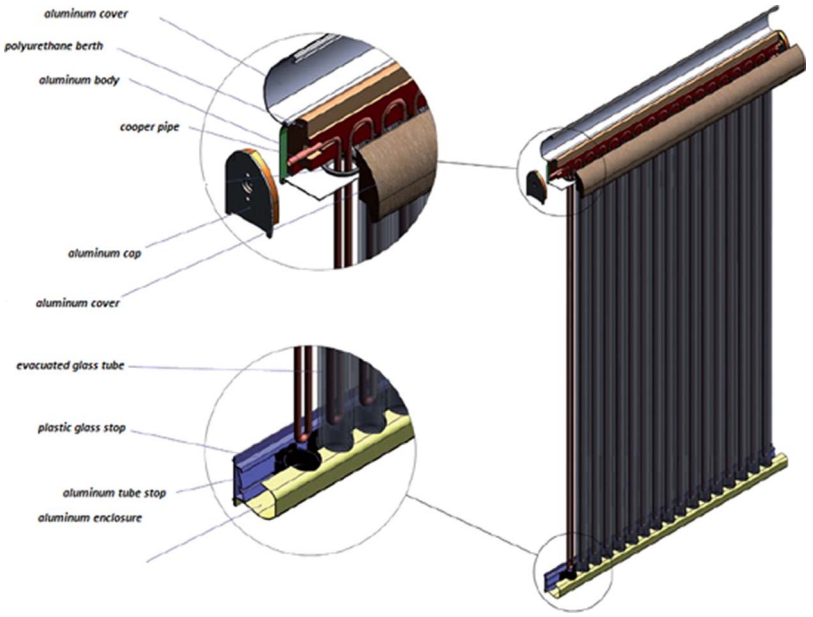

Figure 2. *The schematic shows the internal structure of ETHP.*

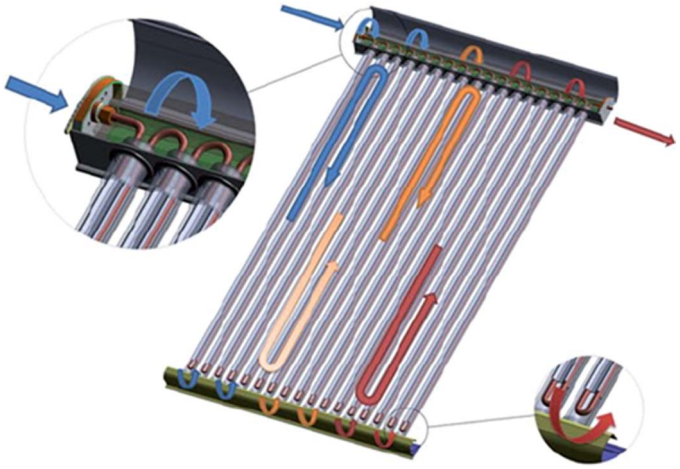

Figure 3. *The schematic shows of the ETHP collector.*

Figure 4. *The ETHP system.*

This section covers some of the critical aspects of thermodynamics in terms of the energy and exergy equations used in the ETHP system. For a steady-flow process, the four balance equations are applied to find the work and heat change, the rate of exergy change, the rate of irreversibility and the energy and exergy efficiencies. The exergy is a form of utilizable quality of energy or potential of the capability to the work. To calculate the exergy, mass balance and energy balance firstly are established when analysing the first law of thermodynamics. The thermodynamic analysis of the ETHP system was investigated by using the Engineering Equation Solver (EES) program. Energy and exergy analysis of the system was performed according to the following formulas.

Total mass balance of the system

$$\sum \dot{m}_i = \sum \dot{m}_e \tag{1}$$

where $\dot{m}_i$ and $\dot{m}_e$ are the mass flow rate of the working fluid at the inlet and outlet of the control volume, respectively.

The energy balance of the system

$$\dot{Q} - \dot{W} = \sum \dot{m}_e h_e - \sum \dot{m}_i h_i \tag{2}$$

where $\dot{Q}$, $\dot{W}$ and h are the heat, work and enthalpy rate of the control volume, respectively.

The exergy balance of the system

$$\sum \dot{m}_i \varepsilon_i + \dot{E}x_Q = \sum \dot{m}_e \varepsilon_e + \dot{E}x_W + \dot{E}x_D \tag{3}$$

In Eq. (3), ε is the specific exergy rate, $\dot{E}x_Q$ is the exergy rate of the heat, $\dot{E}x_W$ is the exergy of the work and $\dot{E}x_D$ is the exergy destruction. The rate of solar energy delivered by ETHP working fluid can be found as shown in Eq. (4):

The solar energy

$$\dot{E}n_{\text{solar}} = I * \rho_{\text{ref}} * \rho_{\text{rec}} * \varepsilon_{\text{rec}} * A \tag{4}$$

where I is the solar radiation, ρ_{ref} is the reflection coefficient of mirrors, ρ_{rec} is an absorber of the receiver, ε_{rec} is the emissivity of the receiver and A is the reflector area. The rate of solar exergy input can be found using Eq. (5):

The solar energy

$$\dot{E}x_{\text{solar}} = \dot{E}n_{\text{solar}} \left(1 + \frac{1}{3}\left(\frac{T_{\text{air}}}{T_{\text{sun}}}\right)^4 - \frac{4}{3}\left(\frac{T_{\text{air}}}{T_{\text{sun}}}\right)\right) \tag{5}$$

where T_{air} is the ambient temperature and T_{sun} is the sun temperature. The net exergy change of water is writer using Eq. (6):

The exergy change of water

$$\dot{E}x_{\text{water}} = \dot{E}x_{\text{out}} - \dot{E}x_{\text{in}} \tag{6}$$

where $\dot{E}x_{\text{out}}$ and $\dot{E}x_{\text{in}}$ are the output water exergy rate and the input water exergy rate, respectively.

The exergy of output water

$$\dot{E}x_{\text{water,output}} = \dot{m} * C_p * \left(\frac{T_{\text{out}}}{T_{\text{air}}}\right) - T_{\text{air}} \left(\ln \frac{T_{\text{out}}}{T_{\text{air}}}\right) \tag{7}$$

where T_{out} is the output water exergy rate.

The exergy of input water

$$\dot{E}x_{\text{water,input}} = \dot{m} * C_p * \left(\frac{T_{\text{in}}}{T_{\text{air}}}\right) - T_{\text{air}} \left(\ln \frac{T_{\text{in}}}{T_{\text{air}}}\right) \tag{8}$$

where T_{in} is the output water exergy rate. The exergy efficiency rate of the ETHP system calculated is shown in Eq. (9):

The exergy efficiency of the ETHP system

$$\eta_{II} = \frac{\dot{E}x_{\text{water}}}{\dot{E}x_{\text{solar}}} \tag{9}$$

The exergy efficiency rate of the ORC system found using Eq. (10):

The exergy efficiency of the ORC system

$$\eta_{II} = \frac{\dot{W}_{\text{Turbine}}}{\dot{E}x_{HE}^{Q}} \tag{10}$$

where $\dot{W}_{\text{Turbine}}$ is turbine work in the ORC system.

2.3. Artificial neural networks

Computer systems that model human intelligence and decision-making processes are called artificial intelligence. As artificial intelligence is developed in electronic systems, it is used in many fields such as banking, agriculture and engineering applications. Artificial intelligence consists of two basic structures: expert systems and artificial neural networks. Artificial intelligence applications that have developed rapidly in the last decade give good results in solving many problems in engineering. Artificial neural networks for engineering applications present current trends especially for the solution of complex engineering problems that cannot be solved through conventional methods. A properly trained neural network is considered to be an 'expert' in the category of information provided for analysis and can then be used to provide projections and answer 'what if' considering new information situations [28]. Especially in neural networks with incomplete data sets or fuzzy logic applications, the accurate modeling and the establishment of the right structures provide a high success rate [29–31]. In the ANN model, the inputs of the system represent the problem given to the model, while the parameters in the output processing section give the calculation results obtained by the neural network (Figure 5). The structure of the model of artificial neural networks is basically composed of three parts. The first one is the network structure of the selected model, the second is the number of hidden layers and the third is the number of neurons. The most commonly used architectures are general regression neural networks (GRNN), probabilistic neural networks (PNN), backpropagation neural network (BPNN) and the group method of data handling (GMDH). The BPNN has been applied with great success to model many phenomena in the field of engineering. Artificial neural networks (ANNs) each neuron in one layer receive inputs from the neurons in the previous layer (a specified or random number) and initiate a training process to adjust the weights of the interconnections between the neurons. It then processes its output through connections to neurons on the other layer. If the value obtained at the output is known, the training will be audited. Therefore, each link is assigned a weight, which is a numerical estimate of the link force [32–34].

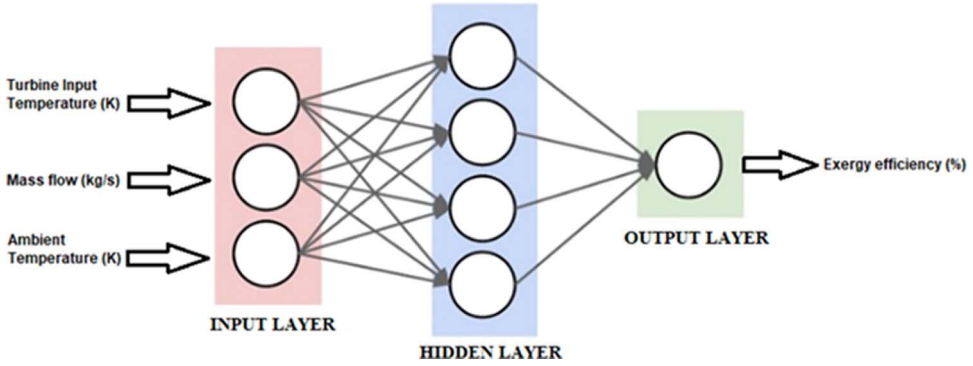

Figure 5. *Schematic diagram of an artificial neural network.*

The developed ANN model allows us to choose which variables will be used as network inputs and outputs and to either specify or compute the minimum and maximum value for each variable. Since the developed ANN model requires variables to be scaled into the range 0 to 1 or 1 to 1, the network needs to know the variable's real value range. For this reason, the minimum and maximum values for each variable are calculated. Besides the training set, also a test set and a production set of data from the training patterns are used. We choose the use the N percent for test set and M percent for the production set as randomly. Also, the recurrent network with input layer feedback is selected as the network architecture of the BPNN model. Suitable neurons are used in the hidden slabs, and the scale function algorithm, the learning rate and momentum impacts are taken as appropriate for our dataset in each tested model.

Large learning rates often lead to oscillation of weight changes and learning never completes, or the model converges to a solution that is not optimum. One way to allow faster learning without oscillation is to make the weight change a function of the previous weight change to provide a smoothing effect. The momentum factor determines the proportion of the last weight change that is added into the new weight change.

In general, the ANN performance of the data sets dealt with is based on some statistical criteria, such as the coefficient of multiple determination (R^2) and the coefficient of variation (r).

The coefficient of multiple determination

$$R^2 = 1 - \frac{\sum (y - \hat{y})^2}{\sum (y - \bar{y})^2} \tag{11}$$

where y is the actual value, $\hat{y}$ is predicted value of y and $\bar{y}$ is the mean of the y values. The formula of the correlation coefficient is defined as follows:

The correlation coefficient

$$r = \frac{n\left(\sum xy\right) - \left(\sum x\right)\left(\sum y\right)}{\sqrt{\left[\ln \sum x^2 - \left(\sum x\right)^2\right]\left[\ln \sum y^2 - \left(\sum y\right)^2\right]}} \tag{12}$$

where n equals the number of patterns, x refers to the set of actual outputs and y refers to the predicted outputs. When the exergy concept is applied to the system examined by ANN analysis, values are converged by thermodynamic modeling. By finding the values, the differences that will occur by making changes on the model that is actually installed without making changes on the system are simulated.

3. RESULTS AND DISCUSSION

In this study, the exergy analysis of the ORC power system integrated into the ETHP system, which is one of the solar energy systems, was performed. The values obtained as a result of the analysis, such as exergy efficiency, are shown in Table 1. Also, these results are modeled with ANN in terms of the sustainability concept. The impacts of some critical shows such as ambient temperature, mass flow rate and turbine inlet temperature and pressure on the exergy efficiency, exergy destruction rate and useful products of the proposed system are analysed. When the turbine inlet temperature is 358 K, the mass flow rate is 0.36 kg/s and the ambient temperature is 280 K, the lowest exergy efficiency is calculated as 17.46%. In contrast, if the turbine inlet temperature is 358 K, the mass flow rate is 0.25 kg/s and the ambient

Table 1. *The result of the thermodynamic analysis of the ETHP system.*

Turbine input temperature (K)	Mass flow (kg/s)	Ambient temperature (K)	Exergy efficiency (%)
323	0.36	294	0.2096
⋮	⋮	⋮	⋮
372	0.36	294	0.2406
358	0.25	294	0.3195
⋮	⋮	⋮	⋮
358	0.397	294	0.2147
358	0.36	280	0.1746
⋮	⋮	⋮	⋮
358	0.36	305	0.3187

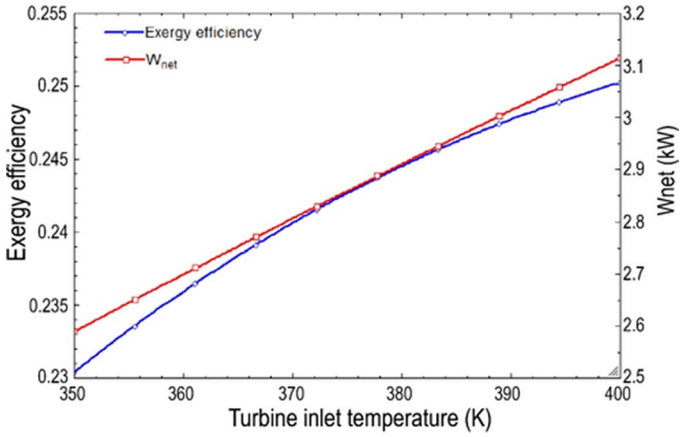

Figure 6. *W_{net} and exergy efficiency of the ORC system according to the turbine inlet temperature.*

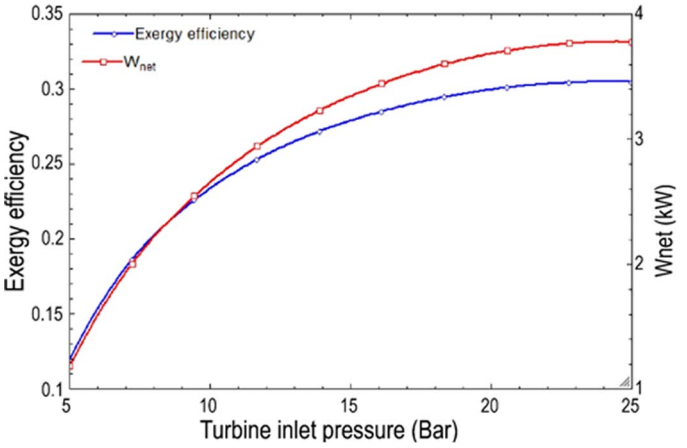

Figure 7. *W_{net} and exergy efficiency of the ORC system according to turbine inlet pressure.*

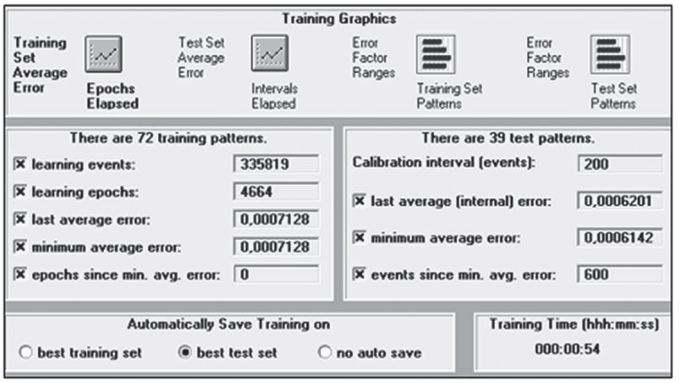

Figure 8. *The training and learning criteria in the developed BPNN models.*

temperature is 294 K, the highest exergy efficiency found is 31.95%. We understand from this table that the ambient temperature is the main effect in the overall system efficiency. Because as the ambient temperature increases, the irreversibility produced from the system will increase depending on the aforementioned value. In this case, it is inevitable that the exergy efficiency obtained from the system will decrease.

In this study, one of the most critical parameters is the ambient temperature. In this study, one of the most critical parameters is the turbine inlet temperature. The performance parameters such as energy and exergy values turbine inlet temperature changed severely depending on the turbine inlet temperature, mass flow rate and solar radiation. Figure 6 shows the assessment of the difference between the exergy efficiency and net produced work of the solar-based ORC system according to the turbine inlet temperature changes. The system thermodynamic parameters of exergy efficiency and net produced work logarithmically increased in parallel with the rising temperature of the turbine inlet. This is due to the increase in unit energy production from the turbine inlet temperature.

Figure 7 shows the impact of the ORC turbine inlet pressure ratio on the exergy efficiency of the investigated cycle and the whole system. As the compression ratio of the turbine inlet pressure rises, the exergy efficiency and net produced work of the system initially increase and then became stable after reaching a peak at about a compression ratio of 22 bar. It can be concluded that this is because more irreversibility occurs in the turbine after the turbine inlet pressure ratio reaches the peak.

The developed ANN model is constructed to evaluate the thermodynamic results of the ORC power system integrated into the ETHP system, exergy efficiency and sustainability. For the backpropagation, general regression neural network architectures are developed. As the GRNN model did not succeed, only the BPNN model's properties and results are given below. The turbine input temperature (K), the mass flow (kg/s) and the ambient temperature (K) are taken as input parameters, and the exergy efficiency (%) is considered as an output parameter in the developed models. In all the developed BPNN models which are BPNN with each layer connected to only the previous layer (standard nets), BPNN with recurrent networks with dampened feedback (Jordan–Elman nets), BPNN with multiple hidden slabs with different activation functions (Ward nets) and BPNN with each layer connected to every previous layer (jumped connection nets) in the learning phase, training and the testing are calculated according to the minimum and last average errors. The last average error from the BPNN algorithm reaches almost zero (0.00006) after approximately 4664 learning epochs (Figure 6).

Different activation functions are tried in these models too. Best results are taken in the logistic (sigmoid logistic) activation function. In the hidden neurons, two neurons participate in the hidden slabs. Pattern selection is rotational and 72 patterns (%55 of the dataset) processed for training, 39 patterns (%30 of the dataset) processed for testing and 19 patterns (%15 of the dataset) processed for forecasting. The learning rates is 0.2; momentum is 0.3 in all the hidden layers. As it can be seen in Figure 8, 4664 training approaches were carried out in order to approach average errors to zero value during the training phase by using 72 patterns. In the test phase, 600 attempts were created with 39 patterns to bring the minimum average error value closer to zero. In the

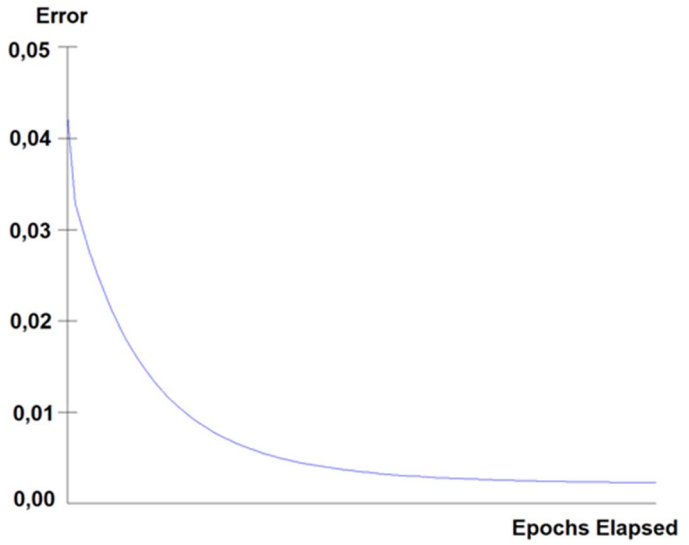

Figure 9. *The epoch–error graph of the developed BPNN (Jumped connection nets).*

Table 2. *Relative contribution (strength) factors of input parameters on the output parameter according to Model 4.*

Input parameters	Strength factors on exergy efficiency
Turbine input temperature (K)	0, 25102
Mass flow (kg/s)	0, 44422
Ambient temperature (K)	0, 50969

developed neural network model, the best training architecture was terminated when the best test result was obtained.

In this study, when the ANN model examined was evaluated using various standard statistical performance evaluation criteria and mathematical formulations trained, in the BPNN training cycle, for the *R* squared value and correlation coefficient, the best is obtained from the BPNN with each layer connected to every previous layer (Jumped connection nets) (Figure 9).

All the BPNN success rates are higher than 95% (0.95), but only at the BPNN with recurrent networks with dampened feedback (Jordan–Elman nets) does an over-learning occur so that the relative contribution (strength) factor results did not become meaningful. On the other hand, according to Model 4 which is BPNN with each layer connected to every previous layer (Jumped connection nets), the relative contribution (strength) factors of input parameters on the output parameter are so meaningful (Table 2).

4. CONCLUSION

The proposed cycle is supported by solar energy, which produces useful outcomes such as electricity. The investigated model comprises two parts: a solar ETHP collector cycle and ORC systems. A detailed thermodynamic performance assessment is applied to identify the exergy performance of this system. In this study, an exergy analysis of the ORC system integrated into the ETHP system, which is one of the methods of utilization of solar energy, was modeled with ANN. Equilibrium equations for thermodynamic results are solved by the Engineering Equation Solver (EES) program. The thermophysical results were successfully predicted by ANN with meaningful errors.

The exergy efficiency value of the ORC system integrated into ETHP was estimated depending on the turbine inlet temperature, mass flow and ambient temperature system values as an input by using ANNs. The ANN approach, which is developed, demonstrated to be a meaningful forecast tool. In this sense, it is understood that ANN can be successfully implemented for modeling and forecast in energy systems. This study is expected to contribute to the literature in terms of energy and exergy planning, sustainability, determination of energy policies and exergy efficiency. Some outstanding results obtained from this study can be expressed as follows.

- In this study, it is understood that the estimation of the exergy efficiency of the ETHP system can be obtained with artificial neural network models in highly successful results if there are sufficient data.
- The exergy efficiency of the ORC system integrated into ETHP was calculated as 23.39%.
- Ambient temperature was found to be the most influential parameter on exergy efficiency.
- The output values show that an increase in ambient temperature reduces the exergy efficiency, thus adversely affecting the ORC electricity generation rate.
- The success rate of the developed BPNN model is 95.4%.
- The most suitable BPNN architecture for this case study is recurrent networks with dampened feedback (Jordan–Elman nets).
- It is seen that BPNN is an applicable neural network algorithm to forecast the exergy efficiency of the ORC system integrated into ETHP.
- For future works, better results can be obtained by extending the training and testing datasets.
- This study is expected to contribute to the literature in terms of sustainability and to encourage authorities to apply solar systems to sustainable buildings.

REFERENCES

[1] Yilmaz F. Thermodynamic performance evaluation of a novel solar energy based multigeneration system. *Appl Therm Eng* 2018;**143**:429–37 https://doi.org/10.1016/j.applthermaleng.2018.07.125.

[2] Utlu Z, Onal BS. Thermodynamic analysis of thermophotovoltaic systems used in waste heat recovery systems: An application. *Int J Low-Carbon Tec* 2018;**13**:52–60 https://doi.org/10.1093/ijlct/ctx019.

[3] Hoffmann JE. On the outlook for solar thermal hydrogen production in South Africa. *Int J Hydrog Energy* 2019;**44**:629–40 https://doi.org/10.1016/j.ijhydene.2018.11.069.

[4] Erten, B., Utlu, Z. & Karabuga, A., 2019, Assessment of the hydrogen production system for domestic type use, *4th International Hydrogen Technologies Congress (IHTEC-2019)*, June 20-23, 2019, **1**:102–107 Edirne, Turkey.

[5] International Energy Agency. 2006. *Renewable Energy; RD&D Priorities, Insights from the IEA Technology Programmes*. Paris: IAE.

[6] Huang X, Wang Q, Yang H *et al.* Theoretical and experimental studies of impacts of heat shields on heat pipe evacuated tube solar collector. *Renew Energ* 2019;**138**:999–1009 https://doi.org/10.1016/j.renene.2019.02.008.

[7] Tong Y, Kim J, Cho H. Effects of thermal performance of enclosed-type evacuated U-tube solar collector with multi-walled carbon nanotube/water nanofluid. *Renew Energ* 2015;**83**:463–73 https://doi.org/10.1016/j.renene.2015.04.042.

[8] Ersoz MA. Effects of different working fluid use on the energy and exergy performance for evacuated tube solar collector with thermosyphon heat pipe. *Renew Energ* 2016; **96**:244–56 https://doi.org/10.1016/j.renene.2016.04.058.

[9] Jowzi M, Veysi F, Sadeghi G. Experimental and numerical investigations on the thermal performance of a modified evacuated tube solar collector: Effect of the bypass tube. *Sol Energ* 2019;**183**:725–37 https://doi.org/10.1016/j.solener.2019.03.063.

[10] Elsheniti MB, Kotb A, Elsamni O. Thermal performance of a heat-pipe evacuated-tube solar collector at high inlet temperatures. *Appl Therm Eng* 2019;**154**:315–25 https://doi.org/10.1016/j.applthermaleng.2019.03.106.

[11] Ghritlahre HK, Prasad RK. Application of ANN technique to predict the performance of solar collector systems - a review. *Renew Sust Energ Rev* 2018;**84**:75–88 https://doi.org/10.1016/j.rser.2018.01.001.

[12] Daghigh R, Zandi P. Improving the performance of heat pipe embedded evacuated tube collector with nanofluids and auxiliary gas system. *Renew Energ* 2019;**134**:888–901 https://doi.org/10.1016/j.renene.2018.11.090.

[13] Jayanthi, N., Kumar, S.R., Karunakaron, G. & Venkatesh, M.2019 Experimental investigation on the thermal performance of heat pipe solar collector (HPSC), *Materials Today: Proceedings* (in press). https://doi.org/10.1016/j.matpr.2019.07.607

[14] Li, J., Li, X., Wang, Y. & Tu, J., 2019, A theoretical model of natural circulation flow and heat transfer within horizontal evacuated tube considering the secondary flow, *Renew Energ*, (in press). https://doi.org/10.1016/j.renene.2019.08.135

[15] Hojjat M. Nanofluids as coolant in a shell and tube heat exchanger: ANN modeling and multi-objective optimization. *Appl Math Comput* 2020;**365**:124710 https://doi.org/10.1016/j.amc.2019.124710.

[16] Daniels JW, Heymsfield E, Kuss M. Hydronic heated pavement system performance using a solar water heating system with heat pipe evacuated tube solar collectors. *Sol Energ* 2019;**179**:343–51 https://doi.org/10.1016/j.solener.2019.01.006.

[17] Iranmanesh M, Akhijahani HS, Jahromi MSB. CFD modeling and evaluation the performance of a solar cabinet dryer equipped with evacuated tube solar collector and thermal storage system. *Renew Energ* 2020;**145**:1192–213 https://doi.org/10.1016/j.renene.2019.06.038.

[18] Tolon FE, Karabuga A, Tolon M, Utlu Z. Evaluation of thermodynamic analysis of solar energy systems integrated into sustainable buildings with artificial neural network: A case study. *Procedia Comput Sci* 2019;**158**:91–8 https://doi.org/10.1016/j.procs.2019.09.031.

[19] Shahverdi K, Loni R, Ghobadian B *et al.* Energy harvesting using solar ORC system and Archimedes screw turbine (AST) combination with different refrigerant working fluids. *Energ Convers Manage* 2019;**187**:205–20 https://doi.org/10.1016/j.enconman.2019.01.057.

[20] Facão F, Palmero-Marrero A, Oliveira AC. Analysis of a solar assisted micro-cogeneration ORC system. *Int J Low-Carbon Tec* 2008;**3**:254–64 https://doi.org/10.1093/ijlct/3.4.254.

[21] Jiradi M, Li J, Liu H, Riffat S. Micro-scale ORC-based combined heat and power system using a novel scroll expander. *Int J Low-Carbon Tec* 2014;**9**:91–9 https://doi.org/10.1093/ijlct/ctu012.

[22] Wei L, Ma Z, Gong X, Guo X. Experimental investigation and performance analysis of an organic Rankine cycle for low-temperature heat to electricity generation. *Int J Low-Carbon Tec* 2019;**14**:500–7 https://doi.org/10.1093/ijlct/ctz037.

[23] Selbas R, Yilmaz F. Thermodynamic analyses and sustainability assessment of solar-based organic Rankine cycle. *Int J Exergy* 2016;**19**:91–109. doi: 10.1504/IJEX.2016.074269.

[24] Yakut MZ, Karabuga A, Kabul A, Selbas R. Design, energy and exergy analyses of linear Fresnel reflector, exergetic, energetic and environmental dimensions. *Book Chapter* 2018;**1**:523–32 https://doi.org/10.1016/B978-0-12-813734-5.00029-9.

[25] Karabuga A, Utlu Z, Selbas R. Examination of the liquefaction system for the use of different cryogenics in terms of thermodynamic analysis. *Int J Exergy* 2019;**29**:1–21. doi: 10.1504/IJEX.2019.099701.

[26] Utlu Z, Hepbasli A. Parametrical investigation of the effect of dead (reference) state on energy and exergy utilization efficiencies of residential–commercial sectors: A review and an application. *Renew Sust Energ Rev* 2007;**11**:603–34 https://doi.org/10.1016/j.rser.2005.05.002.

[27] Utlu Z, Hepbasli A. Comparison of Turkey's sectoral energy utilization efficiencies between 1990 and 2000, part 1: Utility and industrial sectors. *Energy Sources* 2010;**26**:1331–44 https://doi.org/10.1080/00908310490441629.

[28] Awodele O, Jegede O. Neural networks and its application in engineering. *Proceedings of Informing Science & IT Education Conference (InSITE)* 2009;**1**:83–95.

[29] Vafaei LE, Sah M. Predicting efficiency of flat-plate solar collector using a fuzzy inference system. *Procedia Computer Science* 2017;**120**:221–228 https://doi.org/10.1016/j.procs.2017.11.232.

[30] Keskinbora KH. Medical ethics considerations on artificial intelligence. *J Clin Neurosci* 2019;**64**:277–82 https://doi.org/10.1016/j.jocn.2019.03.001.

[31] Al-Mufti F, Dodson V, Lee J *et al.* Artificial intelligence in neurocritical care. *J Neurol Sci* 2019;**404**:1–4 https://doi.org/10.1016/j.jns.2019.06.024.

[32] Tolon M. 2007. A neural network approach for slope stability during Earthquake. In *Master's Thesis*. Istanbul, Turkey: Faculty of Civil Engineering, Istanbul Technical University.

[33] Marugan, A.P., Marguez, F.P.G., Perez, J.M.P. & Ruiz-Hernandez, D. A survey of artificial neural network in wind energy systems, *Appl Energ* 2018;**228**:1822–1836. https://doi.org/10.1016/j.apenergy.2018.07.084

[34] Demirezen G, Fung SA. Application of artificial neural network in the prediction of ambient temperature for a cloud-based smart dual fuel switching system. *Energ Proced* 2019;**158**:3070–5 https://doi.org/10.1016/j.egypro.2019.01.992.